

# A COMPARISON OF POWER FLOW, FULL AND FAST DYNAMIC SIMULATIONS

Alessandro Manzoni

Glauco N. Taranto

Djalma M. Falcão

Federal University of Rio de Janeiro - COPPE  
21940-970 - Rio de Janeiro, RJ - Brazil

**Abstract** – This paper presents a comparative voltage stability study performed in a reduced model of the Southern Brazilian power system using a power flow, a fast dynamic simulator, and a full dynamic simulator. In the fast simulator, the fast dynamics are neglected in the calculation of the time trajectories but the full dynamic model is kept represented for bifurcation analysis. The fast simulator is able to identify *Saddle Node* bifurcations, as well as *Hopf* and *Singularity-Induced* bifurcations, and to deal with large-scale power system models. The results shown in the paper indicate that the results of the fast dynamic simulator are consistent with the ones obtained with the full time domain simulator.

**Keywords:** *Bifurcations, Long-Term Simulation, Voltage Stability*

## 1 INTRODUCTION

Voltage stability is a main concern in modern interconnected power system operational and expansion planning. Heavy loaded systems presenting weak reactive support in certain areas may experience voltage collapse for some contingencies. Voltage instability may occur in transient (few seconds) or in mid- and long-term time frames (several minutes). The first phenomenon is mainly due to the fast acting load and control apparatus like induction motor loads, HVDC links, etc. The second one is the result of slow-acting control devices like LTC transformers, generator overexcitation limiters (OEL), thermostatically controlled loads, etc.

Transient voltage stability is closely associated with electromechanical transient stability and is usually analyzed using time domain simulation. Mid- and long-term voltage stability, on the other hand, may be studied using load flow models as well as time domain simulation. Load flow models are attractive owing to their relatively small computational requirements and simpler data sets. However, it does not properly model the chronological effects of the slow acting controls. Recently, a simulation method in which fast transient phenomena, not directly influencing mid- and long-term voltage stability has been proposed [1,2]. This method, referred to in this paper as fast simulation, keeps the computational advantage of the load flow models while properly modeling the dynamics relevant to mid- and long-term voltage stability studies.

Sole reliance on static models for voltage stability assessment has been not recommended as these models

may produce results conducive to wrong conclusions regarding stability margins. A recent paper [3] has shown significant discrepancies between the results achieved in voltage stability studies conducted for an area of the USA power system using static models and full time domain simulations. It can be shown that the static model can only detect the so-called *Saddle Node* bifurcation, which is associated with the maximum static transmission limit, and identified in the popular nose curve as the critical point. This type of bifurcation is associated with a monotonically decaying of the voltage in a bus or group of busses. However, an analysis of the dynamic model of the power system reveals that other types of bifurcation may occur. For instance, the *Hopf*, which causes a form of oscillatory voltage instability, and *Limit Induced* bifurcations may occur under certain load conditions and have been identified in actual voltage incidents [4-7].

This paper presents a comparative voltage stability study performed in a reduced model of the Southern Brazilian power system using a power flow, a fast dynamic simulator, and a full dynamic simulator. The fast dynamic simulator used in the studies is based on an enhanced version of the method reported in [1]. In this new version, the full dynamic model is kept represented for bifurcation analysis only. The simulation, however, is performed using the same ideas of [1], i.e., the fast dynamics are neglected. The fast simulator is able to identify both *Saddle Node* and *Hopf* bifurcations and to deal with large-scale power system models. The results shown in the paper indicate that the results of the fast dynamic simulator are consistent with the ones obtained with the full time domain simulator.

## 2 METHODOLOGIES

The three methodologies compared in this paper for voltage stability analysis are briefly described in this section.

### 2.1 Load Flow

The usual procedure followed by electric utilities for loadability limit determination is through the use of a conventional load flow program. The process consists in submitting the system to a gradual load increase, following a determined load increase pattern, up to an operating point in which the system reaches the maximum transfer capability in some transmission corridor. Several methods to detect this point have been proposed

in the literature [4,8], most of them are associated with the determination of the singularity of the Jacobian matrix of the load flow equations, or matrices derived from it, that relates the non convergence of the load flow algorithm with the critical point. Among the indices used to indicate the proximity to the point of singularity of the Jacobian matrix, the most used are the condition number, the minimum singular value, the minimum eigenvalue, etc.

In this paper, it is assumed that the system loadability limit is given by the point in which it is not possible to obtain convergence in the load flow solution process, after a sequence of solution points reached through a gradual increase in the load from an initial base case. Although the authors acknowledge that this criterion does not give exactly the point in which the Jacobian matrix reaches singularity, the results obtained through the monitoring of the minimum eigenvalue of the load flow Jacobian matrix show that the difference between the exact value and this approximation present no significant difference and, therefore, does not change qualitatively the presented results.

## 2.2 Full Dynamic Simulation

Full dynamic simulation, usually referred to generically as time domain simulation, is the methodology that gives the more precise answer to the power system dynamical behavior. For that reason, it is always used whenever a detailed study of the dynamical phenomenon is required. Also, it can be used as a benchmark to validate the results obtained with other methodologies.

The full dynamic simulation consists in the numerical solution of the nonlinear set of differential and algebraic equations (DAE) describing the system dynamical behavior:

$$\begin{aligned} \dot{x} &= f(x, y) \\ 0 &= g(x, y) \end{aligned} \quad (1)$$

where  $x$  is the vector of state variables, such as rotor speed and angle,  $y$  is the vector of algebraic variables, such as the complex nodal voltages, and  $f$  and  $g$  are vectors of non-linear functions describing, respectively, the differential equations modeling the system dynamical elements (generators and their controllers, FACTS devices, induction motors, etc.) and the algebraic equations modeling the network.

In the full dynamic simulation, the set of differential equations is algebraized through a numerical integration method (usually the implicit trapezoidal rule) and, then, lumped with the algebraic equations and solved step-by-step along the time trajectory.

In mid- and long-term simulations, i.e., simulations from a few seconds up to some hours, it is required to model devices and control systems with slower actuation time that are generally neglected in transient stability studies. Modeling of devices like overexcitation limiters (OEL), and the centralized controllers like automatic generation control and secondary voltage control, should be included in the simulation. The same applies to discrete action devices like load tap changers

(LTC), capacitors and reactors switching and the demand curve itself. The whole set of equations to be considered in this case is:

$$\begin{aligned} \dot{x} &= f(x, y, z_{(k)}) \\ 0 &= g(x, y, z_{(k)}) \\ z_{(k+1)} &= h(x, y, z_{(k)}) \end{aligned} \quad (2)$$

where  $z$  is the vector of discrete action variables and  $h$  is the vector of control functions.

Although the full dynamic simulation can reproduce fairly exactly the dynamic behavior of the system, its computer requirements are generally too high for long-term simulations. Moreover, it does not easily give information regarding sensitivities and the degree of system instability. The determination of the local and probable cause of the system instability usually requires the analysis of a large number of curves and simulations.

## 2.3 Fast Dynamic Simulation

The phenomena involved in the voltage stability studies are usually of slow nature being driven by the action of discrete type devices and load variation. Thus, the transient dynamics may be neglected and substituted by the equilibrium equation:

$$0 = f(x, y, z_{(k)}) \quad (3)$$

This fact was in the origin of a simulation method based on the quasi-steady-state approximation of the long-term dynamics [1,2] and referred to in this paper as the Fast Dynamic Simulation (FDS) method. The method consists in the calculations of a succession of equilibrium points along the system trajectory determined by the condition of the load and discrete control variables. The Newton method is used to calculate the new equilibrium point through the solution of the following set of equations:

$$\begin{aligned} 0 &= f(x, y, z_{(k)}) \\ 0 &= g(x, y, z_{(k)}) \\ z_{(k+1)} &= h(x, y, z_{(k)}) \end{aligned} \quad (4)$$

The new equilibrium point is, then, used to check whether any discrete variable needs to be updated. This happens, for instance, when the error in the voltage controlled by an LTC violates its limit requiring that the tap position to be moved one step in order to correct the voltage deviation. Therefore, in this simulation method, the system dynamics is governed by the load evolution and the action of the discrete controls devices ( $z_{(k+1)}$ ).

The assumption of the transient dynamics being instantaneous and stable (3) makes unnecessary the use of a numerical integration method. This fact, together with the usually smooth load variation and simplifications introduced in the modeling of the dynamically represented components (a generator and its controllers represented by three state variables only, for instance), make this simulation method computationally very efficient.

However, the approximations introduced in the dynamical models make the FDS, as described above, unsuitable for the detection of some dynamical phenomena of oscillatory nature like *Hopf* bifurcation, for instance. For that reason, in the following section of the paper it is introduced a modification in the FDS in order to make it suitable for the detection of this kind of phenomena.

### 3 ENHANCED FAST DYNAMIC SIMULATION

The modeling of the quasi-steady-state simulator, as given in [9], has some assumptions that not only simplifies the differential equations but also eliminates state variables that do not influence in the equilibrium point, e.g., state variables associated with power system stabilizers. The proposed enhanced version of the Fast Dynamic Simulator (EFDS) does not make any of these simplifying assumptions. Therefore, if necessary, the EFDS is able to capture all dynamics modeled in (1).

The following simplistic example highlights the main difference between both propositions:

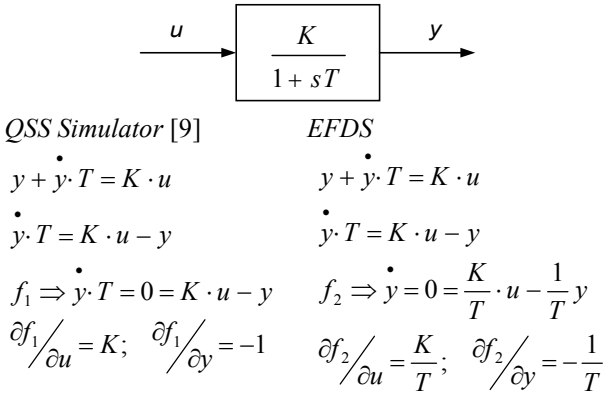


Figure 1: QSS Simulator vs. EFDS

Fig. 1 shows that in the QSS Simulator the time constant  $T$  remains in the left-hand side of equation  $f_1$  whereas in the EFDS it is moved to the right-hand side of equation  $f_2$ . This implies that the coefficients resulting from the linearization of  $f_2$ ,  $(\partial f_2/\partial x; \partial f_2/\partial y)$  retain the information associated with variable  $T$  (time constants of the system).

In terms of equilibrium point, both simulators rigorously achieve the same point. However the EFDS formulation retains the full dynamics of the system and, in addition, all associated modal information.

The linearization of (1) yields:

$$\begin{bmatrix} \dot{\Delta x} \\ 0 \end{bmatrix} = \underbrace{\begin{bmatrix} \frac{\partial f}{\partial x} & \frac{\partial f}{\partial y} \\ \frac{\partial g}{\partial x} & \frac{\partial g}{\partial y} \end{bmatrix}}_{J_{xy}} \cdot \begin{bmatrix} \Delta x \\ \Delta y \end{bmatrix} \quad (5)$$

The Jacobian matrix  $(J_{xy})$ , associated with the proposed EFDS is the Jacobian matrix of the descriptor system utilized in the analysis of small-signal stability. The system eigenvalues can either be obtained from  $J_{xy}$  [10], or from the State Matrix given below

$$A = \begin{bmatrix} \frac{\partial f}{\partial x} \\ \frac{\partial f}{\partial y} \end{bmatrix} - \begin{bmatrix} \frac{\partial f}{\partial x} \\ \frac{\partial f}{\partial y} \end{bmatrix} \times \begin{bmatrix} \frac{\partial g}{\partial y} \\ \frac{\partial g}{\partial x} \end{bmatrix}^{-1} \times \begin{bmatrix} \frac{\partial g}{\partial y} \\ \frac{\partial g}{\partial x} \end{bmatrix} \quad (6)$$

The eigenvalues of  $A$  determines the local stability for the whole spectrum modeled in (1). Tracking the system eigenvalues along the trajectory reveals different types of local bifurcations such as, *Hopf*, *Saddle-Node*, *Singularity Induced*, *Node Focus*, *Limit Induced*, etc. Moreover, valuable pieces of information, such as eigenvector sensitivities, participation factors and mode shapes are readily available. This information may be used for tuning of controllers and for indication of effective remedial actions.

Compared to the Jacobian matrix used in [1-2,9], the Jacobian matrix  $(J_{xy})$  used in this paper may be of a much larger dimension, particularly if highly detailed models for generators and controlling devices are used. However, the larger dimension of  $(J_{xy})$ , does not significantly deteriorates the computational performance, since the large computational effort is to factorize the submatrix  $(\partial g/\partial y)$ , associated with the network algebraic equations, which is basically the same in both methods.

## 4 RESULTS

The methodologies were applied to a reduced model of the South Brazilian System, comprised of 45 busses, 56 transmission lines, 17 transformers (6 LTCs) and 10 generators, as shown in the one-line diagram given in the Appendix. The total system base load is 6473 MW and 942 Mvar.

The results were obtained using a software, namely *FastSim<sup>++</sup>*, that uses advanced concepts of Object-Oriented Modeling (MOO) in C<sup>++</sup>. The computational platform integrates a continuation power flow, the fast simulator (EFDS) and a full simulator to the same data base. This feature greatly enhances the ability to analyze non-trivial phenomena associated with local bifurcations of the DAE (1).

### 4.1 Modeling and Objectives

The simulation objective is to compare the maximum loadability point achieved for the cases of using the load flow equations, the fast simulation and the full simulation. Follow below how the simulations were performed in the cases of the:

- **Load Flow:** the generating busses are represented by P $\theta$  and PV (with reactive power limits either enforced or ignored). All loads in the system face an increment of 1%, maintaining constant the power factor until non-convergence of the load flow equations. All generators equally pick up the loads.
- **EFDS:** the generators are represented by a 5<sup>th</sup> order model, the AVRs by a 2<sup>nd</sup> order model and the speed governors by a 2<sup>nd</sup> order model. The loads face a positive ramp of 5% rate per minute, until non-convergence of (1) is reached.
- **Full Simulation:** identical to the EFDS setup.

The reactive power limits ( $Q_{min}$  and  $Q_{max}$ ), in the load flow, and the field voltage ( $E_{fd}$ ), in the fast and full simulation, were adjusted to generate the same amount of reactive power at 1.0 pu of terminal voltage. To simplify the analysis, the LTCs were not allowed to change their tap position along the simulations. Although important in the voltage instability mechanism, the LTC with automatic tap changing could blur some points that the authors would like to emphasize.

#### 4.2 Determination of the Stability Margin

This subsection presents a comparison of the stability margin determined by the load flow, the fast simulator and the full simulator. Tables 1 and 2 show the results in terms of the percentage of load increase with respect to the base case load.

Methodology	Maximum Loadability	
	Without limits	With limits
Load Flow	41%	13%
Fast Simulator	24%	7%
Full Simulator	12%	8%

**Table 1:** Maximum Loadability for Constant Power Load Model (Active and Reactive: 100% P)

Methodology	Maximum Loadability	
	Without limits	With limits
Load Flow	55%	18%
Fast Simulator	50%	17%
Full Simulator	47%	19%

**Table 2:** Maximum Loadability for the following load model (Active: 60% P + 40% Z, Reactive: 100% Z)

Tables 1 and 2 show that the Load Flow gives optimistic results when compared to the fast simulator, with a percentage difference varying from 1% (Table 2 – with limits) to 17% (Table 1 – without limits).

Tables 1 and 2 also show an apparent inconsistency when comparing the full and the fast simulators. The fast simulator gives a larger margin when the field voltage limits are neglected and a smaller margin when those limits are enforced.

A more comprehensive analysis of the results shown in Tables 1 and 2, comparing firstly the Fast Simulator vs. the Load Flow and secondly the Fast Simulator vs. the Full Simulator, is presented in the following subsections.

#### 4.3 Fast Simulation vs. Load Flow

A comparative analysis of some variables helps to explain the differences in Tables 1 and 2. Figure 2 shows the terminal voltages and the reactive power output of two generators (J. Lacerda and P. Fundo). The simulation reveals that J. Lacerda reaches its limit.

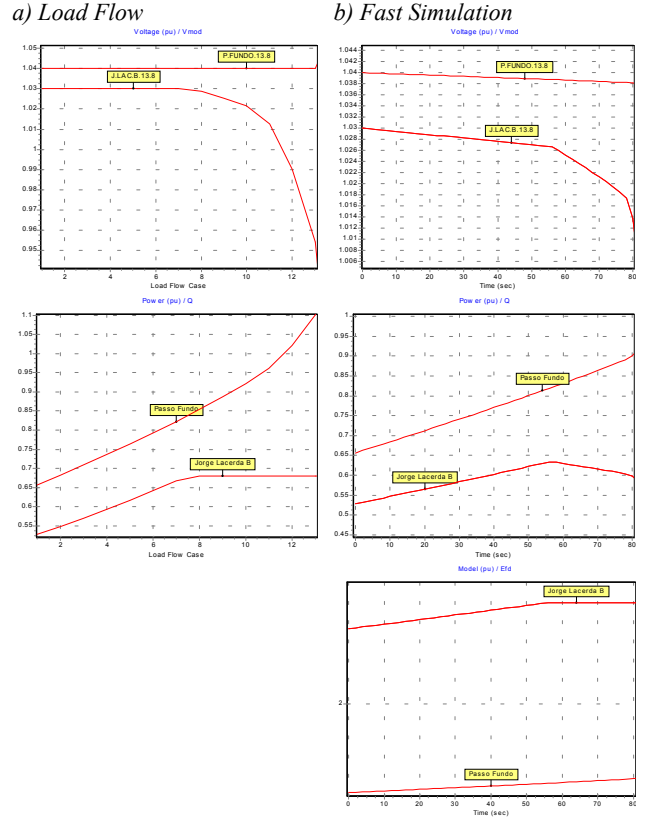


**Figure 2:** Load Flow vs. Fast Simulation

In the Load Flow, the terminal voltages (PV busses) remain constant while the reactive power limit is not reached. When this happens, the reactive power output is kept constant and the terminal voltage depresses.

In the Fast Simulator, the generators follow their droop characteristics, and the voltage depresses a little even when the field voltage ( $E_{fd}$ ) limit is not reached. When this limit is reached, the simulation shows a depression both in the terminal voltage and in the reactive power output, since the latter is dependent of the former. Moreover, this lower voltage profile yields higher reactive losses in the system.

#### 4.4 Fast Simulation vs. Full Simulation

For the sake of clarity some results of Tables 1 and 2 are expressed in Tables 3 and 4 as time to instability for the same positive load ramp.

Methodology	Time to Instability (seconds)	
	Without limits	With limits
Fast Simulation	295	86
Full Simulation	145	102

**Table 3:** Instability detection for constant power load model (Active and Reactive: 100% P)

Methodology	Time to Instability (seconds)	
	Without limits	With limits
Fast Simulation	600	207
Full Simulation	553	235

**Table 4:** Instability detection for the following load model (Active: 60% P + 40% Z, Reactive: 100% Z)

Apparently Tables 3 and 4 show inconsistencies as in the case when limits are ignored, the full simulation detects instability first, whereas, in the case when the limits are forced, the fast simulation detects the instability first. In order to explain these results a more detailed analysis is shown below.

#### 4.4.1 Case A: Limits Ignored

Due to space limitation, only the case of load with constant power model will be shown. The instantaneous recovery of the loads do not substantially change the point the authors want to make, since only small positive steps of load are applied at each integration step of the full simulation. The conclusions are valid for the other load modeling.

Figures 3 and 4 show the bus voltages and the reactive power output obtained by the Fast Simulator and by the Full Simulator, respectively.

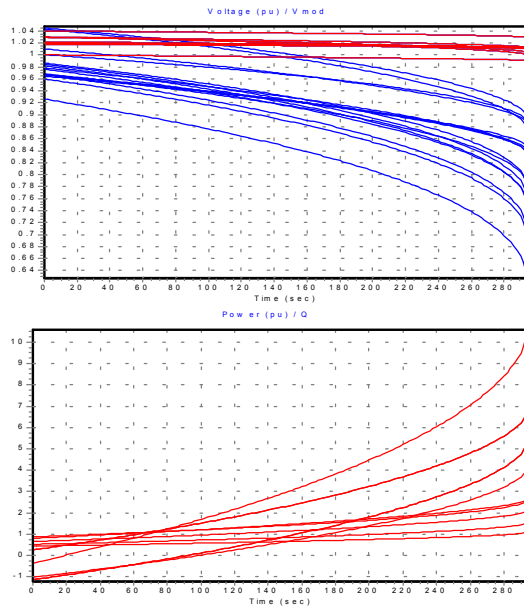


Figure 3: Fast Simulation

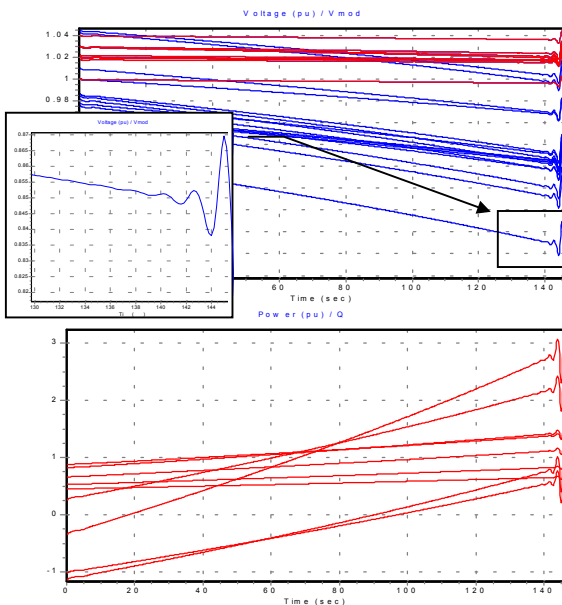


Figure 4: Full Simulation

While the fast simulator detects instability only at 295 sec (non convergence), instability can be observed in the full simulator at 142 sec, as shows by the undamped oscillations in Fig. 4.

However the proposed EFDS allows the analysis of the system eigenvalues along the time trajectory. Figure 5 shows the tracking of the system eigenvalues along the time simulation.

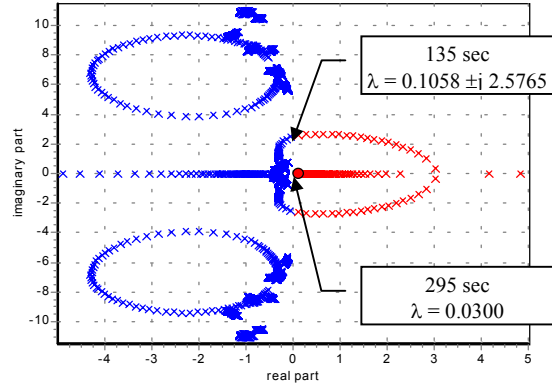


Figure 5: Eigenvalue locus ( $\lambda$ )

The system eigenvalues show that, although the singularity of the state matrix (non convergence) occurs at  $\approx 295$  sec ( $\lambda \rightarrow 0.0$  – Saddle-Node Bifurcation), at  $\approx 135$  sec the system undergoes an unstable equilibrium point ( $\lambda \rightarrow 0.0 \pm j 2.5765$  – Hopf Bifurcation). This finding corroborates the result obtained by the full simulation (see enlarged view in Fig. 4).

#### 4.4.2 Caso B: Limits Enforced

Figures 6 and 7 show the bus voltages and the reactive power output obtained with the Fast Simulation and with the Full Simulation, respectively.

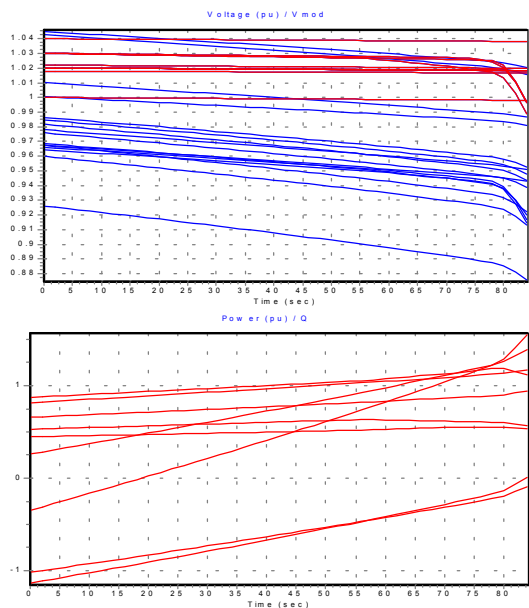
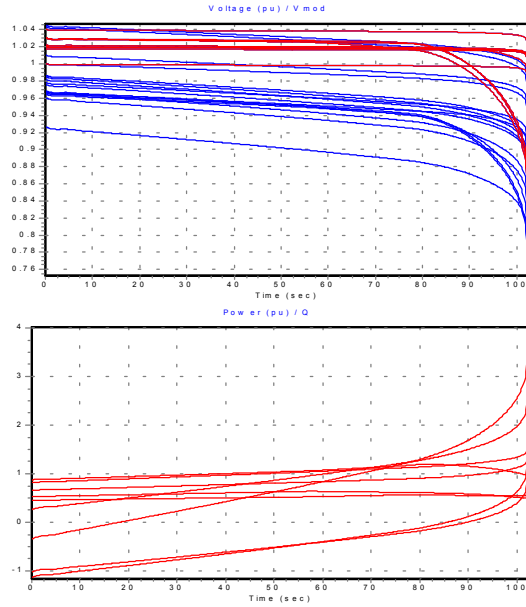


Figure 6: Fast Simulation with Limits Enforced



**Figure 7:** Full Simulation with Limits Enforced

In this case the fast simulator detects instability before the full simulator, using the criterion of non convergence of the system equations.

Figure 8 shows the eigenvalues loci along the system trajectory. The system equations do not converge at  $\approx 86$  sec as  $\lambda \rightarrow 0.0$  (Saddle-Node Bifurcation).

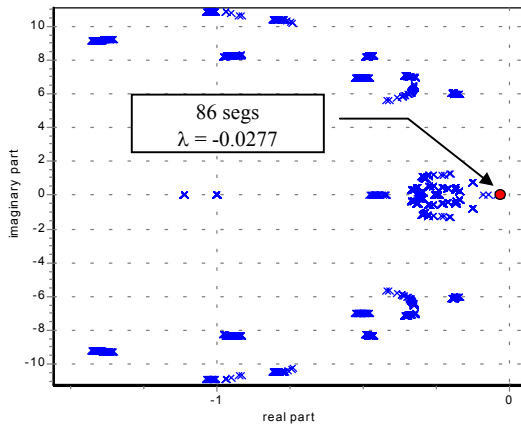


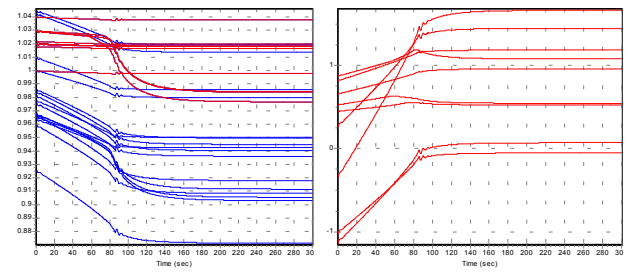
**Figure 8:** Eigenvalue Locus

In order to clarify the system behavior, two additional full simulations were performed:

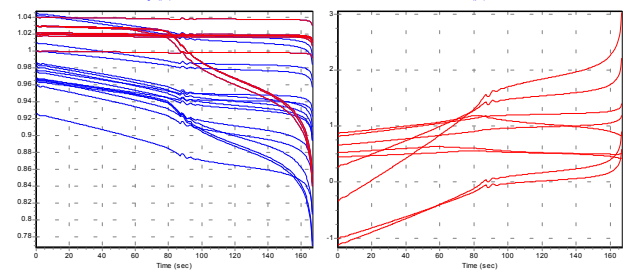
- The load ramp is applied until 86 sec, remaining constant from this point on;
- The load ramp is applied until 87 sec, remaining constant from this point on.

Figure 9.a shows the bus voltages and the reactive power outputs for the first simulation. The system remains stable throughout the simulation. Figure 9.b shows the bus voltages and the reactive power outputs for the second simulation. In this case the system becomes unstable.

**a) Load ramp applied until 86 sec – STABLE SYSTEM**



**b) Load ramp applied until 87 sec – UNSTABLE SYSTEM**



**Figure 9:** Additional Simulations

The results presented in Fig. 9, reveal that, although instability is detected only at 102 sec by the full simulation (Fig. 7), the system is already unstable at 87 sec, when one system eigenvalue becomes zero. This delay can be explained by the existing inertia of the system and by the actuation of the system controllers.

#### 4.5 Correction to the Stability Margins

The new maximum loadability point of the system, give by the Fast Simulator, was modified by the analysis of the eigenvalues (Figures 5 and 8). Under this new viewpoint the maximum load, that maintains the system stable, is obtained when the first eigenvalue becomes unstable.

The new loadability points (stability margins) are given in Tables 5 and 6.

Methodology	Maximum Loadability	
	Without limits	With limits
Load Flow	41%	13%
Fast Simulator	<b>11%</b>	<b>7%</b>
Full Simulator	12%	8%

**Table 5:** Modified maximum loadability for constant power model (Active and Reactive: 100% P)

Methodology	Maximum Loadability	
	Without limits	With limits
Load Flow	55%	18%
Fast Simulator	<b>45%</b>	<b>17%</b>
Full Simulator	47%	19%

**Table 6:** Modified maximum loadability for the following load model (Active: 60% P + 40% Z, Reactive: 100% Z)

## 5 CONCLUSIONS

The comparison of the load flow with the fast simulator indicates that the analysis based only on load flow models may lead to optimistic results. The discrepancies are influenced by the load model and by the limits.



The simulations shown in the paper indicate that the results of the enhanced fast dynamic simulator are consistent with the ones obtained with the full time domain simulator.

The obtained results reveal that the proposed EFDS combines short computational time with the ability to detect instabilities along the system trajectory. There is a tradeoff between speed and precision, since the calculation of the eigenvalues increases the overall computational time. However, the utilization of methods that calculate the dominant spectrum mitigates this problem.

### REFERENCES

- [1] T. Van Cutsem, Y. Jacquemart, J.N. Marquet, P. Pruvot, "A Comprehensive Analysis of Mid-Term Voltage Stability", *IEEE Transactions on Power Systems*, Vol. 10, pp. 1173-1182, 1995.
- [2] T. Van Cutsem, C.D. Vournas, "Voltage Stability Analysis in Transient and Mid-Term Time Scales", *IEEE Transactions on Power Systems*, Vol. 11, pp. 1173-1182, 1996.
- [3] B.H. Chowdhury, C.W. Taylor, "Voltage Stability Analysis: V-Q Power Flow Simulation Versus Dynamic Simulation", *IEEE Transactions on Power Systems*, Vol. 15, pp. 1354-1359, 2000.
- [4] C. Cañizares, ed., "Voltage Stability Assessment, Procedures and Guides," IEEE/PES Power System Stability Subcommittee Special Publication, Final Draft, January 2001, available at [www.power.uwaterloo.ca](http://www.power.uwaterloo.ca).
- [5] A. A. P. Lerm, C. A. Cañizares, F. A. B. Lemos, and A. S. e Silva, "Multi-parameter Bifurcation Analysis of Power Systems," *Proceedings of the North American Power Symposium*, Cleveland, Ohio, October 1998.
- [6] V. Venkatasubramanian, H. Schättler and J. Zaborszky, "Local Bifurcations and Feasibility Regions in Differential-Algebraic Systems," *IEEE Transactions on Automatic Control*, Vol. 40, No. 12, pp. 1992-2013, December 1995.
- [7] C. Rajagopalan, B. Lesieutre, P.W. Sauer, M.A. Pai, "Dynamic Aspects of Voltage/Power Characteristics", *IEEE Transactions on Power Systems*, Vol. 7, pp. 990-1000, 1992.
- [8] C. W. Taylor, *Power System Voltage Stability*, New York, McGraw-Hill, 1994.
- [9] T. Van Cutsem, C.D. Vournas, *Voltage Stability of Electric Power Systems*, Norwell, MA, Kluwer, 1998.
- [10] N. Martins, "Efficient Eigenvalue and Frequency Response Methods Applied to Power System Small-Signal Stability Studies," *IEEE Transactions on Power Systems*, Vol. 1, No. 1, pp. 217-226, February 1986.

### APPENDIX

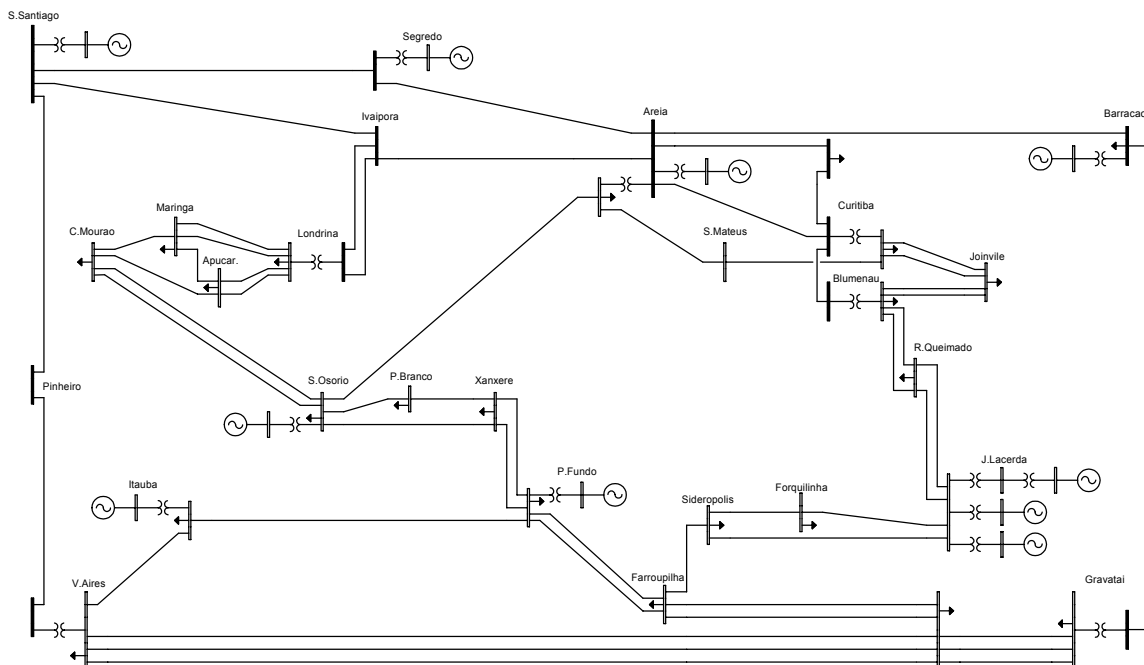


Figure 10: One-line Diagram of the Reduced South Brazilian System